Progress in Biomaterials (2022) 11:67–77
https://doi.org/10.1007/s40204-022-00180-z

ORIGINAL RESEARCH

A hyaluronic acid/PVA electrospun coating on 3D printed PLA scaffold for orthopedic application

Mina Farsi[1] · Azadeh Asefnejad[1] · Hadi Baharifar[2]

Received: 29 November 2021 / Accepted: 5 January 2022 / Published online: 22 January 2022

Abstract

The need for bone tissue replacement, repair and regeneration for orthopedic application is constantly growing. Therefore, the application of cartilage substitute due to the lack of donors as well as biocompatibility leads to immune system rejection. In order to overcome these drawbacks, researchers have used porous scaffold as an option for bone transplantation. In this study, poly-lactic acid (PLA) scaffolds were prepared for cartilage application by fused deposition modeling (FDM) technique and then coated by electrospinning with polyvinyl alcohol (PVA) and hyaluronic acid (HLA) fibers. Hybrid electrospinning (ELS) method was used to produce porous scaffolds from HLA–PVA polymers. The printed scaffold was coated using FDM technique and the mechanical and biological investigation was performed on the polymeric composite specimen. The functional group and morphological behavior were investigated using Fourier-transform infrared spectroscopy (FTIR) and scanning electron microscopy (SEM) techniques. The obtained porous scaffold has hydrophilic properties as the PVA and HLA were coated on the PLA. The porous 3D-printed scaffold containing PLA/PVA/HLA scaffold does not show any toxicity in MTT evaluation after 1, 3 and 7 days. The SEM image confirmed the cell adhesion of the chondrite to the scaffold. Also, the mechanical performances of the sample, such as elastic modulus and compressive strength, were evaluated by compression test. By electro-spun coating, the elastic module of PVA/PLA and PLA/PVA/HLA scaffolds has increased to 18.31 ± 0.29 MPa and 19.25 ± 0.38 MPa. Also, the tensile strength of these two porous scaffolds has reached 6.11 ± 0.42 MPa and 6.56 ± 0.14 MPa, respectively. The failure strain of 3D printed PLA scaffold was reported to be $53 \pm 0.21\%$ and this value was reduced to $47 \pm 0.62\%$ and $42 \pm 0.22\%$ in PVA/PLA and PLA/PVA/HLA scaffolds. The cells' growth on the porous scaffolds showed a broad, spindle-shaped and regular shape. The obtained results of the chemical, physical and biological analyses showed that porous PLA/PVA/HLA scaffold has potential applications in cartilage construction.

Keywords Poly-lactic acid · Polyvinyl alcohol · Hyaluronic acid · 3D printing · Tissue engineering

Introduction

Articular cartilage acts should tolerate a load-bearing, shock-absorbing, and function as a lubricant in the joints, covering the junction of the long bones (Bomhard et al. 2013; Sowmya et al. 2020; Pandey et al. 2020). Cartilage tissue is covered with synovial fluid, which is rich in oxygen, nutrients, and encloses the synovial membrane around the joint (Sowmya et al. 2020; Pandey et al. 2020; You et al. 2021; Danaboina et al. 2020). The chondrocytes cells can lead to more cell growth on the cartilage tissue. The intercellular tissue is a thin fiber, called fibrils, and cartilage tissue is very similar to tissues containing calcium ions and silicate ions. The primary function of cartilage is to control the structure of surrounding tissues as well as to prevent friction against external forces (Pandey et al. 2020; You et al. 2021; Danaboina et al. 2020; Chung and Burdick 2008). Cartilage diseases such as osteoarthritis are among the most common skeletal diseases due to joint wear among the old people as well as athletes. Joint injuries lead to pain, fragility, limited mobility, and tissue swelling which needs to be treated by a surgeon (Danaboina et al. 2020). Articular chondrocytes proliferate slowly in the external environment and rapidly lose their differentiation (Park et al. 2004;

✉ Azadeh Asefnejad
asefnejad@srbiau.ac.ir

[1] Department of Biomedical Engineering, Science and Research Branch, Islamic Azad University, Tehran, Iran

[2] Department of Medical Nanotechnology, Applied Biophotonics Research Center, Science and Research Branch, Islamic Azad University, 1477893855 Tehran, Iran

Sakaguchi et al. 2005; Awad et al. 2004; Garcia-Fuentes et al. 2009). Traumatic injuries, congenital anomalies, and age-related diseases can lead to cartilage loss. These losses include a decrease in thickness, cell density, mitotic divisions, a change in the concentration, size and distribution of proteoglycans. All these changes affect the mechanical properties of the porous tissue. Therefore, there may be a need to remedy a damaged cartilage. Many surgical procedures have been performed to solve the problem of cartilage defects, including debridement or washing of cartilaginous wounds, abrasive arthroplasty, and autologous chondrocyte transplantation (Sakaguchi et al. 2005; Awad et al. 2004; Garcia-Fuentes et al. 2009; Ansari and Alshahrani 2019; Ansari 2015). However, the problem is the open joint surgery which requires to transplant local chondrocytes [6–9]. In addition, the favorable results of the native chondrocyte transplantation technique lead to the loss of cartilages in the body due to an invasive procedure (Garcia-Fuentes et al. 2009). Therefore, due to the high number of patients with joint injuries in the world and the urgent need for this treatment, it is necessary to seriously study the cartilage scaffolds in tissue engineering applications. Many researchers study artificial cartilage tissue as a simple tissue because it is produced with cell, collagen and ceramic component (Alwan et al. 2021; Abid et al. 2021; Okamoto and John 2013; Ghahramani and Javanmardi 2021; Ghahramani et al. 2021; Othman et al. 2019). The hydrophilic environment of the extracellular matrix (ECM), due to its negative charge, enables the tissue to withstand the pressure of swelling against the compression strength. However, there are no available data and techniques to treat the cartilage problem and disease using various compositions with heterogeneous shape. The geometry of the cartilage substitute is difference in layer thickness, cell morphology and composition depending on the depth of the articular cartilage (Ansari and Alshahrani 2019; Ansari 2015; Alwan et al. 2021; Abid et al. 2021). The cell growth process should be in the direction of tissue regeneration in three dimensions basis (Okamoto and John 2013; Ghahramani and Javanmardi 2021). Therefore, in practice, each scaffold must have the ability to introduce specific biological and mechanical effects in order to improve cellular behavior. Nowadays, each scaffold is designed based on the properties of its target texture. Choosing the type and material of the scaffold is the most important part of the design and finally the damaged tissue can be replaced. The porous scaffold in tissue engineering is designed to resemble an ECM. Many substances, such as agarose, hyaluronic acid (HLA), poly-lactic-*co*-glycolic acid (PLGA), poly-lactic acid (PLA), poly-glycolic acid (PGA), silk, alginate and fibrin, have been studied by many researchers (Ansari 2015; Alwan et al. 2021; Abid et al. 2021; Okamoto and John 2013; Ghahramani and Javanmardi 2021; Ghahramani et al. 2021; Othman et al. 2019). Using the following natural and synthetic materials can be used to achieve a hybrid porous scaffold with proper mechanical stability and elastic modulus in micro- and nano-sized (Okamoto and John 2013; Ghahramani and Javanmardi 2021; Tolou et al. 2013; Zeylabi et al. 2010). In this research, an attempt is conducted to obtain a biocompatible and efficient scaffold with suitable degradability using 3D printing technique using PLA which coated with an electrospinning (ELS) technique by composition of PVA and HLA. Then, the physical, mechanical, chemical and biological properties of the scaffold may be discussed.

Materials and methods

A fused deposition modeling (FDM) technique was used to print PLA polymer with Quantum 3D machine. Also, a simplified 3D software was used in Science and Research Center to create a base microarchitecture. The materials used in this study included polyvinyl alcohol (PVA, 98% purity, diameter size 100–150 nm) purchased from Merck company, poly-lactic acid (PLA, 98% purity, diameter size 200–300 nm) provided by Iran Chemicals Company and hyaluronic acid (HLA, 98%, purity, 100 nm) purchased from Merck. The constant plate temperature, nozzle temperature 210 °C, and machine speed of 50 mm/s and nozzle diameter 1.75 mm in the process of 3D printing was set. It is obvious that for PLA polymer the 3D table temperature can be varied from 55 °C to 85 °C. Also, the nozzle temperature which melts the PLA filament was set at 210 °C to 230 °C. The shape was designed in the solid work and inserted into the simplified 3D software connected to the 3D printed machine with the STL format. The shape designed in Solid Works software is in square shape. The designed model has been used because of its proper mechanical properties such as compressive strength. The range of variable print speed increased to 150 mm/s for the machine which decreases to 50 mm/s in this work. After the 3D scaffold was prepared, the 3D scaffold coated with PVA and PVA/HLA fibers. The PVA and HLA used in this study were purchased from Merck Company with high purity. The PVA polymer solution was prepared in a solution of deionized water at 80 °C for 4–5 h at concentrations of 8%, 10% and 12% (by vol). After the preparation of composite solution, the homogeneous solution was gained and its temperature reached an ambient. Then, HLA at 2% (by vol) was added to the solution and placed on a magnetic stirrer for 1 h. This solution was electro-spun at a rate of 0.5 ml/h, a distance of 12 cm to the collector and a voltage of 180 kV. In this method, the injection pump was placed horizontally, and it was connected to a 23-gauge syringe. To induce the load to the solution inside the syringe, the positive pole of the power supply was connected to the syringe. In front of the syringe, a sheet of aluminum (Al) foil was placed on the

collector, which was attached to a 3D printed scaffold as a negative pole of the power supply. In this research, an electrospinning device located in the Faculty of New Medical Technologies was used to make a three-component scaffold. Finally, the fibers were spun randomly onto the fabricated PLA structure.

Fourier-transform infrared spectroscopy (FTIR) analysis

The FTIR analysis was used based on the absorption of radiation and the study of vibrational mutations of molecules and ions of polymer atoms. Some of the information that can be obtained from FTIR including qualitative and quantitative identification of organic compounds containing nanoparticles was detected by the type of functional group and bonds present in the molecules. Also, the FTIR analysis was performed to consider the functional group behavior of polymers after soaking the PLA/PVA/HLA and PLA/PVA sample. In order to investigate the surface functional groups, the FTIR technique was applied (FTIR Ultra shield 400 MHZ, Bruker, Germany) and in the range of 4000–400 cm^{-1} and 2 cm^{-1} resolutions.

Scanning electron microscopy (SEM) analysis

The SEM images were used to investigate the surface and morphological properties of the fabricated nanocomposites. The samples were cut to 1×1 cm dimensions and were covered with gold to increase the electro-conductivity. To evaluate the diameter size and determine the average fiber diameter, 30 sheets of SEM images were selected which measured using Image-J software for porosity evaluation and their standard deviation ($\pm$SD) was reported.

Mechanical properties of the 3D printed scaffold

The mechanical properties of the 3D printed scaffolds coated with electro-spun technique were investigated according to the ASTM D882-10 standard to understand the stress–strain, elastic modulus (slope of stress–strain curve), and the maximum compressive strength value. The tensile strength machine set for this test was an Instron and the sample size was 10 and 30 mm with 10 mm/min speed rate until the fibers were broken up. The test was repeated three times to obtain more valid data and mean standard deviation.

Hydrophilicity of printed scaffolds coated with fibers

The hydrophilicity of the sample was measured by determining the contact angle (wettability) of the water drop on the surface of the fiber. In the evaluation, the sample was placed on a flat surface and a drop of water with a volume of 4 µL was put on the surface of the scaffold. After 20 s, the drop was fixed on the sample and its surface was photographed by a digital camera placed on the device.

Evaluation of degradability of coated 3D printed scaffolds

The specimen was evaluated for weight loss changes according to the ASTM-F1635 standard with size of 1×1 cm in the 5–10 mL of phosphate buffer saline (PBS) solution (pH7.4 and $T = 37$ °C). To measure the weight of the dry and wet samples inside the PBS, the samples were kept in the oven for 24 h. The weights of the samples were measured three time and recorded based on the following formula.

$$\text{Weightloss}(\%) = \frac{W_t - W_d}{W_t} \times 100 \quad (1)$$

where W_t is the dry weight of the sample before immersion in PBS solution and W_d is the dry weight of the sample after soaking in PNS solution.

Chondrocyte cell culture

In this study, Arabbit articular cartilage chondrocytes (RACC) were purchased from Pasteur Institute of Iran. The chondrocytes were cultured in a cell culture flask with DMEM-F12 medium containing 9% Fetal Bovine Serum (FBS) solution and 1% antibiotic (Pen/Str), and the cell-containing flask was incubated in a humid atmosphere containing 5% CO_2 at temperature of 37 °C. A positive control (chondrocyte cell and culture medium) was considered to compare the cell growth rate. The UV-sterilized scaffolds were transferred to a plate with 24 wells and 10^4 cells/100 µL of culture medium. After 1 day, 3 days and 7 days, the adhesion of cells was assessed by MTT method.

MTT assay

At first, the supernatant was removed and the cells were washed twice with PBS solution. Then, 400 µL of culture medium was added to each well and 40 µL of MTT solution was poured inside each. The plates were then placed in an incubator for 4 h. At the end of the incubation period, the culture medium was slowly drained. In this study, 400 µL of dimethyl sulfoxide (DMSO) was added to each plate and after pipetting several times, 100 µL was transferred from each house to plates, and then using ELISA reader, at a wavelength of 570 nm, based on reduced yellow tetrazolium salt, the intensity of light absorption was read. The color of MTT in the mitochondria of living cells changed from yellow to purple, and the concentration of the dye was

a measure of the amount of living cells according to the ISO-10993–5 standard. In order to evaluate the adhesion and morphology of the cells, after 3 days of incubation of the cells on the scaffolds, the culture medium of the samples was emptied. A 3% glutaraldehyde solution was made using distilled water. Then, 500 µL of the solution made in each well of the sample, and incubated for 1 h. Next, it was washed with PBS and diluted with 50% to 100% alcohol. Finally, samples were kept in 100% alcohol to prevent any oxidation before observation by SEM. In order to use SEM image, due to the limitation of the sample in terms of dryness, the samples were placed in the oven to completely dry for proper gold coating.

Statistical studies

All tests were evaluated using SPSS software to examine statistical differences between different scaffold groups and one-way analysis of variance was selected for this purpose.

Result and discussion

Figure 1 shows the microscopic shape of a printed PLA scaffold with the electro-spun PVA/HLA solution in the first 5 s. The 3D printed scaffolds coated with PVA/HLA nanofibers had the dimension of 277.2 ± 27.5 µm. The scaffolds coated with PVA/HLA electro-spun fibers were placed between the printed fibers. The PVA with different concentrations of 8%, 10% and 12% was used for ELS technique. Using the ELS technique at 8% concentration was associated with droplet spraying. The diameters of 10% and 12% PVA nanofibers were 265 ± 29.38 nm and 389.22 ± 12.38 nm, respectively. The porosity of these electro-spun fibers was about 18.21 ± 0.12 and 23.42 ± 0.19, respectively as shown in Table 1. As the concentration of PVA increased, the viscosity also increased which resulted in an increase in fiber diameter and a decrease in porosity. In addition, the fibers had beads in their microstructure, which made the structure of the fibers non-uniform. Therefore, a specific amount of 10% PVA polymer was used as a best solution. Several studies show that in ELS, the fiber diameter depends on the viscosity and electric charge of the solution. In addition, as the viscosity increases, the fiber diameter increases proportionally. The use of 2% (by vol) HLA in the structure of electro-spun fibers with PVA causes the diameter of electro-spun PVA fibers (10%)/HLA to increase from 265 ± 29.38 to 312.4 ± 31.09. This increase in diameter can be due to the addition of HLA in the PVA solution, which leads to an increase in electric charge on the surface of the liquid droplets (Othman et al. 2019). Figure 2 shows the morphology of the electro-spun fibers containing PVA (10%), PVA (12%) and PVA (10%)/HLA on PLA printed scaffold. Figure 3 shows the FTIR spectrum of PLA including CH_3 tensile vibrations at 2829 cm^{-1} and 12,932 cm^{-1} peaks. Also, the OH tensile vibrations are observed in 3501 cm^{-1} and 3667 cm^{-1} (Halim et al. 2020). The tensile vibration C=O also appears in 3501 cm^{-1}. The carbonyl tensile band is specified in 1740 cm^{-1} and the characteristic C–O tensile band is specified in 1010 cm^{-1} (Halim and Ismail 2018). Regarding the FTIR, spectrums of PVA polymer have intermolecular and intramolecular hydrogen bonds (O–H), whose peaks appear within the range of 3550–3200 cm^{-1}. Peaks between 2840 cm^{-1} and 3000 cm^{-1} are observed as a result of C–H tensile bonding of alkyl groups (C_nH_{2n+1}) (Nabishah et al. 1990). Asymmetric C–H asymmetric tensile vibration

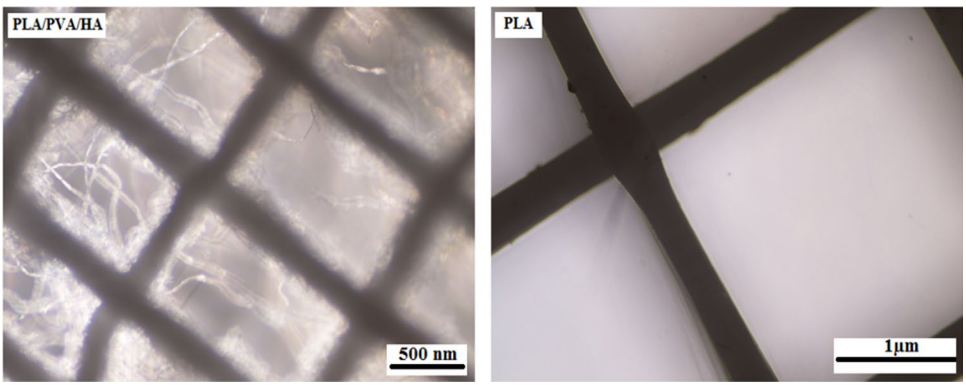

Fig. 1 Microscopic image of 3D printed PLA scaffold and PVA/HLA electrospun on printed PLA scaffold in the first 5 s

Table 1 Properties of electro-spun PVA and PVA/HLA nanofibers

Sample	Elastic modulus (MPa)	Tensile strength (MPa)	Strain break (%)
PLA	17.23 ± 0.45	5.56 ± 0.34	53 ± 0.21
PLA/PVA	18.31 ± 0.29	6.11 ± 0.42	47 ± 0.62
PLA/PVA/HA	19.25 ± 0.38	6.56 ± 0.14	42 ± 0.22

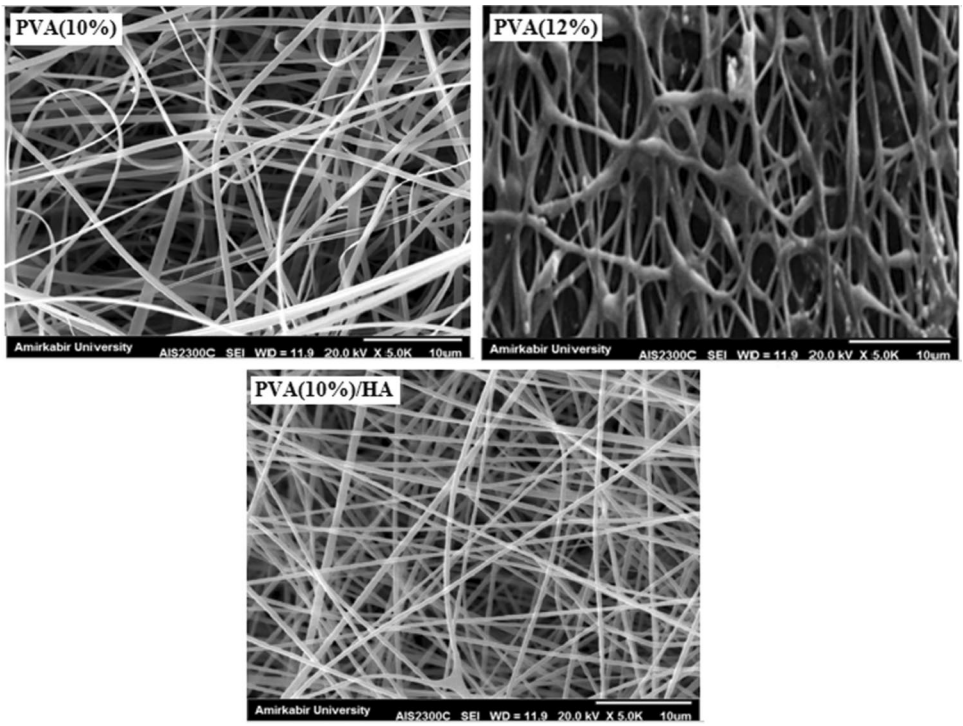

Fig. 2 Electrospun fibers **a** PVA (10%), **b** PVA (12%) and **c** PVA (10%)/HLA on PLA printed scaffold

band occurs at 2926 cm^{-1}. Also, the sharp peaks in 1717 cm^{-1} and 1570 cm^{-1} are due to the presence of the carbonyl group. The sharp band at 1091 cm^{-1} corresponds to the C–O tension of the steel group present in the PVA structure. The peaks shown in 1432 cm^{-1} and 1330 cm^{-1} show CH_2 flexural vibrations (Wardani et al. 2019). The FTIR analysis of the HLA shows that the peak of 1048 cm^{-1} is attributed to the C–O–C tensile bond in HLA. The absorption peaks at 1414 cm^{-1} and 1614 cm^{-1} are assigned to the symmetric and asymmetric tensile vibrations of carboxylic groups (Kaur et al. 2018). Also, characteristic bands C=O in 1603 cm^{-1}, amide bond in 1554 cm^{-1}, CH tensile bond in 2886 cm^{-1}, CH flexural bands in 1405 cm^{-1}, 1374 cm^{-1}, a weak-OH bond in 1312 cm^{-1} and CN tensile bond were recorded at 1248 cm^{-1} (Yang et al. 2018).Table 2 shows the mechanical properties of 3D printed PLA scaffolds, PLA prefabricated scaffolds coated with electro-spun PVA nanofibers and PLA prefabricated scaffolds coated with PVA/HLA electro-spun nanofibers. Increasing the elastic modulus leads to an increase in the tensile strength of the specimens while reducing the fracture strain and decreasing the average fiber size as shown in Table 2. The elastic modulus and tensile strength are reported to be 17.23 ± 0.45 MPa and 5.56 ± 0.34 MPa, respectively. By coating the electrospun fibers, the elastic modulus of PVA/PLA and PLA/PVA/HLA scaffolds has been increased to 18.31 ± 0.29 MPa and 19.25 ± 0.38 MPa. Also, the tensile strength of these two scaffolds has reached 6.11 ± 0.42 MPa and 6.56 ± 0.14 MPa, respectively. The failure strain of 3D printed PLA scaffold was reported to be $53 \pm 0.21\%$ and this value was reduced to $47 \pm 0.62\%$ and $42 \pm 0.22\%$ in PVA/PLA and PLA/PVA/HLA scaffolds. The obtained results indicated that despite the coating of 3D printed PLA scaffolds with electrospun PVA and PVA/HLA nanofibers, a significant increase in the elastic modulus of the scaffolds was observed. The thickness of PVA fiber scaffolds produced by this composition is about 37 µm. In addition, an ideal scaffold should have mechanical properties in accordance with the anatomical location in which it is implanted. The architecture of the 3D scaffold should be strong enough to allow surgery to be implanted (Hein et al. 2020). This study shows that the PVA matrix produced is able to create mechanical stability in the porous scaffolds. A proper scaffold for tissue engineering should have a high hydrophobicity which plays an important role in cell survival, cell growth and proliferation. In this study, the hydrophilicity of the porous coated scaffolds is measured using the wettability method. In this article, water contact angle test was performed for three samples, such as PLA, PLA/PVA and PLA/PVA/HLA scaffolds, according to Fig. 4. Based on previous studies, PLA is a hydrophobic polymer with low hydrophilicity which is due to the presence of methyl groups in the polymer microstructure of PLA polymer. The obtained results of this study demonstrated that the average water contact angle droplets are about $126.2 \pm 28.79°$. Although, PLA polymer is a degradable polymer, its applications in synthetic tissues and organs are limited due to its hydrophobicity, which may lead to weak cell binding (Margiana et al. 2019). As PVA is a hydrophilic

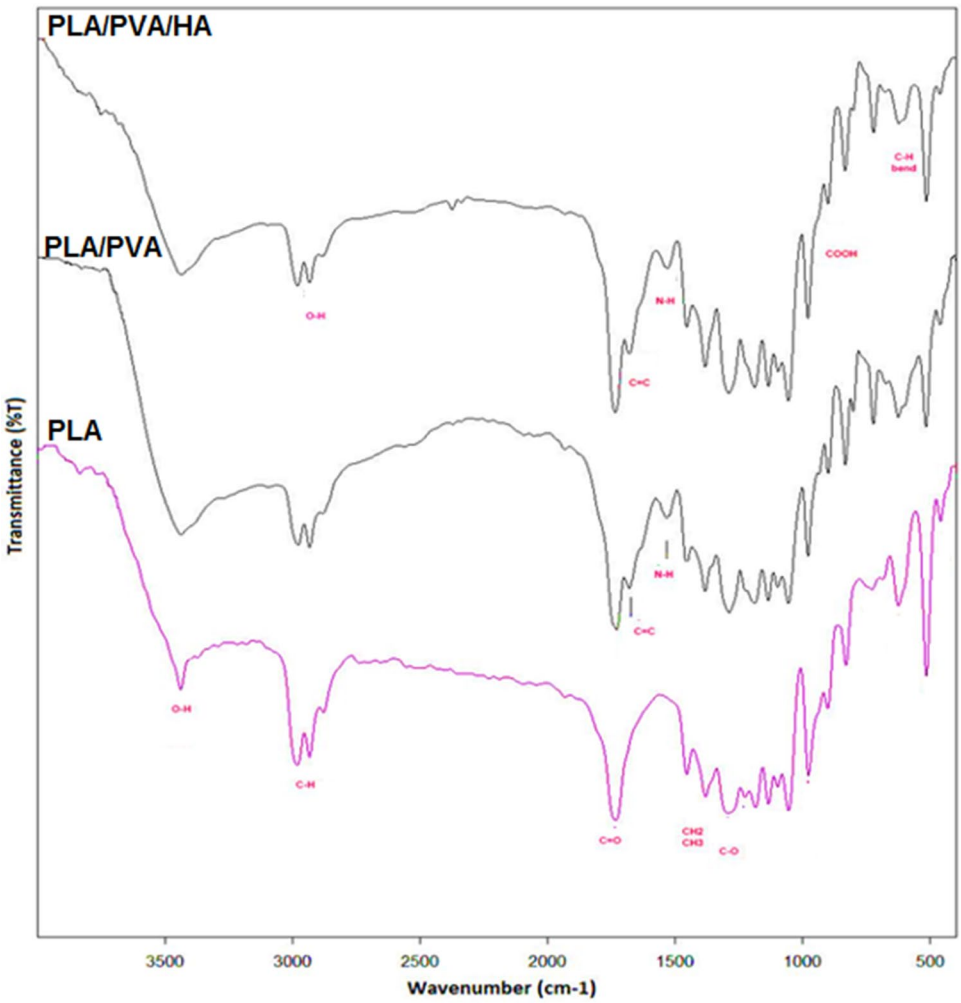

Fig. 3 FTIR spectrum of PLA and PVA/PLA and HA/PVA/PLA scaffolds

Table 2 Investigation of mechanical properties of PLA and PVA/PLA and PLA/PVA/HLA scaffolds

Sample	Average fiber diameter (nm)	Average inter-fiber pore size (micron)
PVA (10%)	93.21 ± 612	0.284 ± 1.734
PVA (12%)	108.11 ± 428	0.401 ± 3.186
PVA (10%)/HLA	37.45 ± 382	0.308 ± 3.674

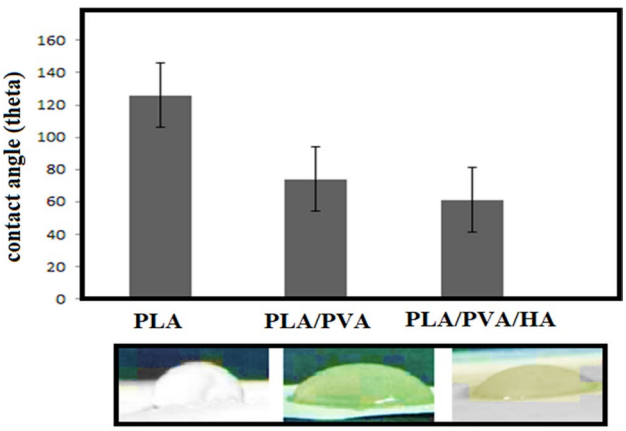

Fig. 4 Contact angle of the PLA, PLA/PVA and PLA/PVA/HLA scaffolds

synthetic polymer, it is expected that by coating the 3D printed PLA scaffold coated with electrospun PVA fibers, the contact angle with water may be reduced, which confirms this statement and the average contact angle is reached to74.38 ± 31.45°. On the other hand, HLA is also hydrophilic by nature that coats the surface of PLA scaffold which leads to a decrease in contact angle and increases in hydrophilicity of the scaffold. In fact, HLA has a complex chemical structure with amine, hydroxyl and carboxyl groups, which leads to higher molecular polarity of the scaffold (Kianfar 2019; Ghadirinejad et al. 2021; Kim et al. 2008; Park et al. 2019; Sun et al. 2021; Karbasian et al. 2021; Raisi et al. 2022; Du et al. 2021; Cheng et al. 2021). Also, the contact angle of PLA/PVA/HLA scaffold was reduced and reached 61.21 ± 21.52° using CCD camera. The pH changes

of the 3D printed PLA scaffold in PBS solution were examined after 8 weeks (pH 7.4). Figure 5 shows no change in the pH of the solution in the first 5 weeks. After 6 weeks, the pH of the solution decreased and the pH reached 6.8. In other words, the PLA scaffold was partially failed and at the end of the 8th week, the pH of the PBS solution reached 6.7. It should be noted that the highest pH changes lead to more destructive event. According to Fig. 6, the 3D printed PLA scaffold lost 15% of its weight at the end of the 8th week when the 3D printed PLA scaffold lost an 8% of its weight in the 6th week by about 12% as shown in Fig. 6. In other words, it can be concluded that in the acidic environment, more degradation occurred in the 3D printed PLA polymer. Figure 6 shows that comparison of the two scaffolds PLA/PVA and PLA/PVA/HA, the destruction was done more quickly and at the end of the 8th week, these two scaffolds lost 39% and 48% of their weight, respectively. Several research studies show that the first degradation mechanism occurs by water absorption process (Raisi et al. 2020; Iranmanesh et al. 2021; Jamnezhad et al. 2020; Salmani et al. 2020b; Bagherifard et al. 2020; Salmani et al. 2020a; Sahmani et al.2019; Aghdam et al. 2020; Shirani et al. 2020; Esmaeili et al. 2019; Khandan et al. 2020; Li et al. 2021; Abasalta et al. 2021; Bagher et al. 2020; Murphy et al. 2020; Razeghian et al. 2021; Jiang et al. 2020). After soaking the samples in PBS solution, the polymer chains begin to weaken due to the separation of the polymer matrix and chemical instability in which the chain is small enough to destroy and begins to decompose (Foroutan et al. 2021). Since, PVA is a hydrophilic polymer, using PVA as coating with electro-spun technique to coat PLA leading to more damage to the scaffold. The 3D printed scaffold made of

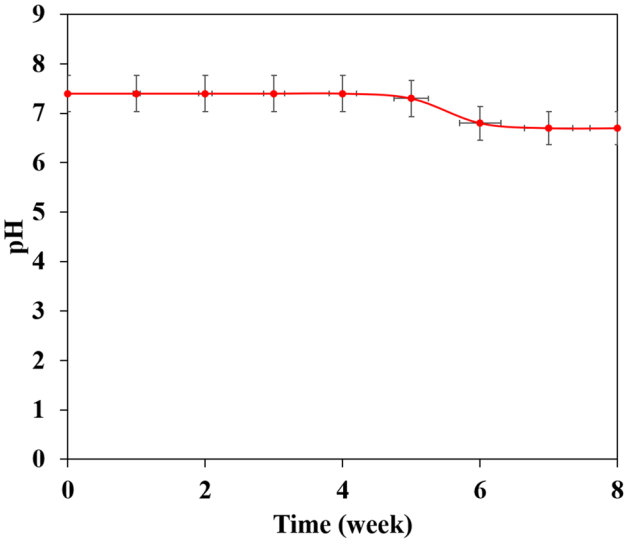

Fig. 5 pH change of PBS solution used for degradation evaluation of PLA porous scaffolds

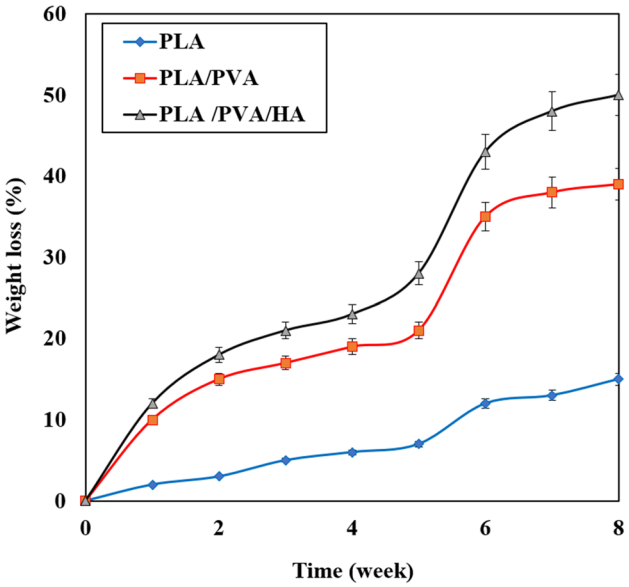

Fig. 6 Degradation diagram of printed PLA, PVA/PLA and PLA/PVA/HA scaffolds

PLA and coated with PVA/HLA leads to more quick degradation rate of the samples. Figure 7 shows the MTT diagram of the sample PLA, PLA/PVA and PLA/PVA/HLA scaffolds without any toxicity compared to the control sample. The chondrocyte cell growth studies showed that better result on 3D printed scaffolds was observed. The MTT experiment showed that the lowest metabolic activity was related to the 3D printed scaffold containing PLA sample. According to the MTT results, it can be said that during the whole experiment, the results were consistent with the cell proliferation method. The scaffold cells containing nanofibers showed greater metabolic activity and more cell proliferation. Kim et al. (2008) fabricate a 3D printed PCL scaffold, and a

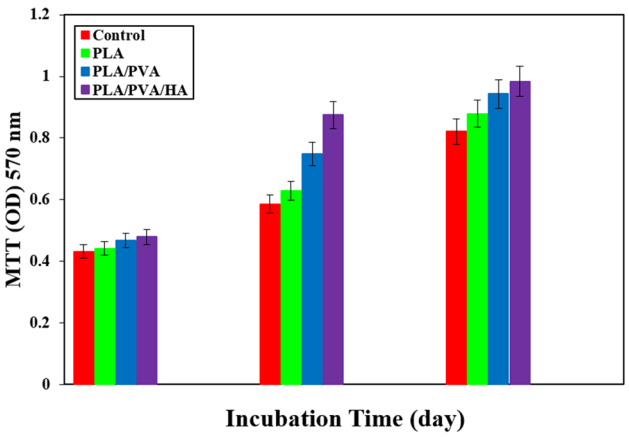

Fig. 7 Diagram of MTT assay on PLA, PVA/PLA and PLA/PVA/HA scaffolds after 1, 4 and 7 days of cell culture ($P \leq 0.05$)

sample coated with PCL nanofibers, the MTT test showed that chondrocytes survived longer on the 3D printed nanocomposite scaffold. These obtained results indicated that the nanofiber architecture can provide a good matrix containing proper adhesion of chondrocyte cells. This would promote rapid and stable tissue formation through cell attachment, cell growth and proliferation (Kim et al. 2008). The MTT test and cell adhesion were performed on two scaffolds PLA/PVA and PLA/PVA/HLA after 3 days. Figure 8 shows the chondrocyte cells growth well on both scaffolds and the chondrocytes adhering to the scaffolds which were completely stretched. The prepared sample using FDM technique made of PLA coated with PVA/HLA has more hydrophilicity, and expected that the cells may show more adhesion on their surface layer compared with the PLA/PVA scaffold. Park et al. (Dong et al. 2021) confirm the role of HLA in the growth, proliferation and adhesion of chondrocytes. The three porous scaffolds with porosity sizes of 500 µm, 700 µm and 900 µm are shown in Fig. 9. According to the results, printed PLA scaffold with lower porosity percentage has higher compressive strength.

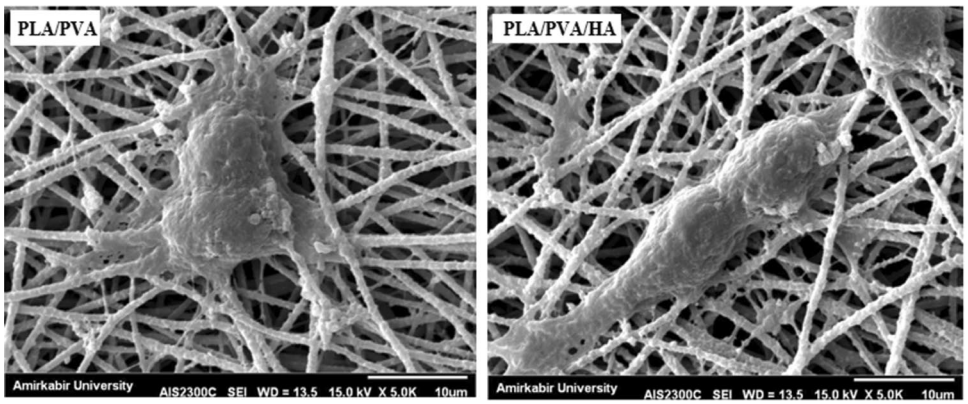

Fig. 8 Chondrocyte cell adhesion of PLA/PVA and PLA/PVA/HLA scaffolds

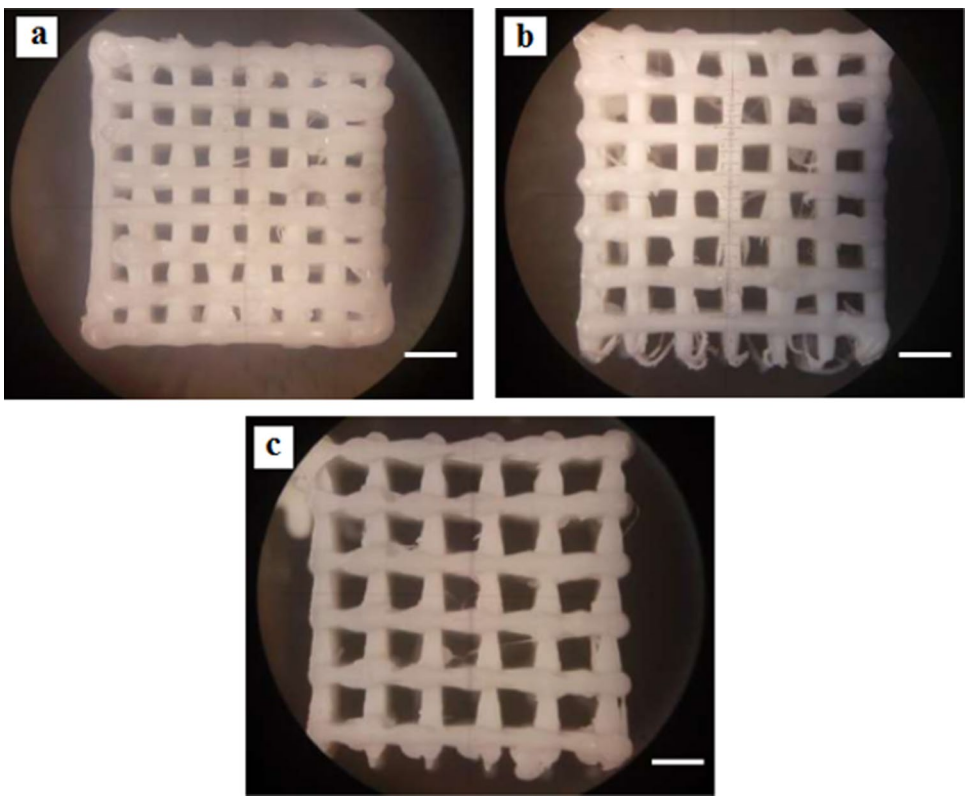

Fig. 9 3D printed PLA scaffolds, **a** porosity size 500 µm, **b** porosity size 700 µm and **c** porosity size 900 µm. (Scale bar: 1 µm)

Conclusion

A novel 3D porous scaffold made of PLA was fabricated using FDM technique and coated with electro-spun method containing PVA/HLA nanocomposite. The prepared scaffold demonstrated various positive qualities, including controlled pore size, mechanical properties, improved chondrocyte cells attachment and proliferation. It has been found that PLA/PVA/HLA nanocomposite scaffold exhibited good cell growth behavior and increased ability for cell attachment. Therefore, the new 3D printed composite scaffold coated with ELS nanofiber with potential application can be a suitable candidate for tissue engineering with excellent mechanical, surface wetting, and cyto-compatibility properties. By coating using electro-spun, the elastic module of PVA/PLA and PLA/PVA/HLA scaffolds has been increased to 18.31 ± 0.29 MPa and 19.25 ± 0.38 MPa. Also, the tensile strength of these two porous scaffolds has reached 6.11 ± 0.42 MPa and 6.56 ± 0.14 MPa, respectively. The failure strain of 3D printed PLA scaffold was reported to be $53 \pm 0.21\%$ and this value was reduced to $47 \pm 0.62\%$ and $42 \pm 0.22\%$ in PVA/PLA and PLA/PVA/HLA scaffolds. The use of 2% (by vol) HLA in the structure of electro-spun fibers with PVA causes the diameter of electro-spun PVA fibers (10%)/HLA to increase from 265 ± 29.38 to 312.4 ± 31.09.

Acknowledgements The authors would like to extend their gratitude for the support provided by Department of Biomedical Engineering, Science and Research Branch, Islamic Azad University, Tehran, Iran.

Funding None.

Data availability Not applicable.

Declarations

Conflict of interest The authors report no conflicts of interest in this work.

Ethical approval and consent to participate Not applicable.

Consent for publication All authors read and approved the final manuscript and consented to publication. Availability of data and materials: No data were used from internet data sources.

References

Abasalta M, Asefnejad A, Khorasani MT, Saadatabadi AR (2021) Fabrication of carboxymethyl chitosan/poly (ε-caprolactone)/doxorubicin/nickel ferrite core-shell fibers for controlled release of doxorubicin against breast cancer. Carbohydr Polym 257:117631

Abid H, Abid Z, Abid S (2021) Atherogenic indices in clinical practice and biomedical research: a short review: atherogenic indices and cardiovascular diseases. Baghdad J Biochem Appl Biol Sci 2(02):59–69

Aghdam HA, Sanatizadeh E, Motififard M, Aghadavoudi F, Saber-Samandari S, Esmaeili S, Sheikhbahaei E, Safari M, Khandan A (2020) Effect of calcium silicate nanoparticle on surface feature of calcium phosphates hybrid bio-nanocomposite using for bone substitute application. Pow Technol 361:917–929

Alwan S, Al-Saeed M, Abid HJBJOB, Sciences AB (2021) Safety assessment and biochemical evaluation of biogenic silver nanoparticles (using bark extract of *C. zeylanicum*) in *Rattus norvegicus* rats: safety of biofabricated AgNPs (using Cinnamomum zeylanicum extract). Baghdad J Biochem Appl Biol Sci 2(03):138–150

Ansari MJ (2015) Investigations of polyethylene glycol mediated ternary molecular inclusion complexes of silymarin with beta cyclodextrins. J Appl Pharm Sci 5:26–31

Ansari MJ, Alshahrani SM (2019) Nano-encapsulation and characterization of baricitinib using poly-lactic-glycolic acid co-polymer. Saudi Pharm J 27(4):491–501

Awad HA, Wickham MQ, Leddy HA, Gimble JM, Guilak F (2004) Chondrogenic differentiation of adipose-derived adult stem cells in agarose, alginate, and gelatin scaffolds. Biomaterials 25(16):3211–3222

Bagher Z, Ehterami A, Safdel MH, Khastar H, Semiari H, Asefnejad A, Davachi SM, Mirzaii M, Salehi MJ (2020) Wound healing with alginate/chitosan hydrogel containing hesperidin in rat model. J Drug Deliv Sci Technol 55:1379

Bagherifard A, JoneidiYekta H, Akbari Aghdam H, Motififard M, Sanatizadeh E, GhadiriNejad M, Esmaeili S, Saber-Samandari S, Sheikhbahaei E, Khandan A (2020) Improvement in osseointegration of tricalcium phosphate-zircon for orthopedic applications: an in vitro and in vivo evaluation. Med Biol Eng Comput 58:1681–1693

Bomhard AV, Veit J, Bermueller C, Rotter N, Staudenmaier R, Storck K, The HN (2013) Prefabrication of 3D cartilage contructs: towards a tissue engineered auricle–a model tested in rabbits. PloS One 8(8):

Cheng Y, Morovvati M, Huang M, Shahali M, Saber-Samandari S, Angili SN, Nejad MG, Shakibaie M, Toghraie D (2021) A multilayer biomimetic chitosan-gelatin-fluorohydroxyapatite cartilage scaffold using for regenerative medicine application. J Mater Res Technol 14:1761–1777

Chung C, Burdick JA (2008) Engineering cartilage tissue. Adv Drug Deliv Rev 60(2):243–262

Danaboina KK, Neerati P (2020) Evidence-based P-glycoprotein inhibition by green tea extract enhanced the oral bioavailability of atorvastatin: from animal and human experimental studies. J Nat Sci Biol Med 11(2):105

Dong X, Heidari A, Mansouri A, Hao WS, Dehghani M, Saber-Samandari S, Khandan A (2021) Investigation of the mechanical properties of a shapeless electroconductive scaffold: addition of akermanite nanoparticles and using a freeze-drying technique. J Mech Behav Biomed Mat 10464:121

Du X, Dehghani M, Alsaadi N, Nejad MG, Saber-Samandari S, Toghraie D, Su C-H, Nguyen HC (2021) A femoral shape porous scaffold bio-nanocomposite fabricated using 3D printing and freeze-drying technique for orthopedic application. Mat Chem Phy 275:125302

Esmaeili S, Shahali M, Kordjamshidi A, Torkpoor Z, Namdari F, Samandari SS, GhadiriNejad M, Khandan A (2019) An artificial blood vessel fabricated by 3D printing for pharmaceutical application. Nanomed J 6(3):183–194

Foroutan S, Hashemian M, Khosravi M, Nejad MG, Asefnejad A, Saber-Samandari S, Khandan A (2021) A porous sodium alginate-$CaSiO_3$ polymer reinforced with graphene nanosheet: fabrication and optimality analysis. Fiber Polym 22(2):540–549

Garcia-Fuentes M, Meinel AJ, Hilbe M, Meinel L, Merkle HP (2009) Silk fibroin/hyaluronan scaffolds for human mesenchymal stem cell culture in tissue engineering. Biomaterials 30(28):5068–5076

Ghadirinejad N, Nejad MG, Alsaadi N (2021) A fuzzy logic model and a neuro-fuzzy system development on supercritical CO2 regeneration of Ni/Al2O3 catalysts. J CO2 Utilization 54:106

Ghahramani Y, Javanmardi N (2021) Graphene oxide quantum dots and their applications via stem cells: a mini-review. Adv Appl NanoBio-Technol 2(3):54–56

Ghahramani Y, Fallahinezhad F, Afsa M (2021) Graphene Quantum Dots And Their Applications: a mini-review. Adv Appl NanoBio-Technol 2:53–59

Halim S, Ismail UU (2018) Potential therapeutic effects of olea Europaea (olive) fruit oil as neuroprotective agent against neurotoxicity induced opioid. J Cell Mole Anesthes 3(4):159–159

Halim S, Jasmi NA, Ridzuan P, Anna D, Abdullah S, Sina T, MEDICINE L (2020) Novel potential *Centella asiatica* extract in ameliorating neurotoxicity induced oxidative stress in chronic morphine dependant rat model. Int J Med Toxic Leg Med 23(3and4):79–83

Hein TC, Muz B, Ahmadi-Montecalvo H, Smith T (2020) Associations AMONG ACEs, health behavior, and veteran health by service era. Am J Health Behav 44(6):876–892

Iranmanesh P, Ehsani A, Khademi A, Asefnejad A, Shahriari S, Soleimani M, Nejad MG, Saber-Samandari S, Khandan A (2021) Application of 3D bioprinters for dental pulp regeneration and tissue engineering (porous architecture). Transp Porous Media. https://doi.org/10.1007/s11242-021-01618-x

Jamnezhad S, Asefnejad A, Motififard M, Yazdekhasti H, Kolooshani A, Saber-Samandari S, Khandan A (2020) Development and investigation of novel alginate-hyaluronic acid bone fillers using freeze drying technique for orthopedic field. Nanomed Rese J 5(4):306–315

Jiang S, Guo W, Tian G, Luo X, Peng L, Liu S, Sui X, Guo Q, Li X (2020) Clinical application status of articular cartilage regeneration techniques: tissue-engineered cartilage brings new hope. Stem Cells Int. https://doi.org/10.1155/2020/5690252

Kaur N, Khan J, Kaleemullah M, Al-Dhalli S, Budiasih S, Florence M, Faller E, Asmani F, Yusuf E, Takao KJIJOMT, Yusuf E, Medicine L (2018) Synthesis of cinnamic acid amide derivatives and the biological evaluation of A-glucosidase inhibitory activity. Int Med Toxicol Leg Med 21(3):216–220

Khandan A, Nassireslami E, Saber-Samandari S, Arabi N (2020) Fabrication and characterization of porous bioceramic-magnetite biocomposite for maxillofacial fractures application. Dent Hypotheses 11(3):74

Kianfar E (2019) Nanozeolites: synthesized, properties, applications. J Sol-Gel Sci Technol 91(2):415–429

Kim G, Son J, Park S, Kim W (2008) Hybrid process for fabricating 3D hierarchical scaffolds combining rapid prototyping and electrospinning. Macro Rap Commun 29(19):1577–1581

Li X, Saeed S-S, Beni MH, Morovvati MR, Angili SN, Toghraie D, Khandan A, Khan A (2021) Experimental measurement and simulation of mechanical strength and biological behavior of porous bony scaffold coated with alginate-hydroxyapatite for femoral applications. Comp Sci Technol 214:1973

Margiana R, Kusumaningtyas S, Lestari SW, Mukdisari Y, Ima K (2019) Review on cyclic adenosine monophosphate signaling pathway (cAMP), DLK signaling pathway, RAS/RAF signaling, retinoic acid signaling, phosphatidylinositol 3-kinase (PI3K) as the signaling pathways involved in peripheral neuronal generation. J Glob Pharm Technol 11(1):181–198

Murphy MP, Koepke LS, Lopez MT, Tong X, Ambrosi TH, Gulati GS, Marecic O, Wang Y, Ransom RC, Hoover MY (2020) Articular cartilage regeneration by activated skeletal stem cells. Nat Med 26(10):1583–1592

Nabishah B, Merican Z, Morat P, Alias A, Khalid B (1990) Effects of steroid hormones pretreatment on isoprenaline-induced cyclic adenosine 3', 5'-monophosphate in rat lung. Gen Pharm 21(6):935–938

Okamoto M, John B (2013) Synthetic biopolymer nanocomposites for tissue engineering scaffolds. Prog Poly Sci 38(10–11):1487–1503

Othman Z, Khalep HRH, Abidin AZ, Hassan H, Fattepur S (2019) The anti-angiogenic properties of *Morinda citrifolia* L. (Mengkudu) leaves using chicken chorioallantoic membrane (CAM) assay. Pharmacogn J 11(1):12–15

Pandey RK, Shukla S, Hadi R, Husain N, Islam MH, Singhal A, Tripathi SK, Garg R (2020) Kirsten rat sarcoma virus protein overexpression in adenocarcinoma lung: Association with clinicopathological and histomorphological features. J Carcino 19:9

Park SS, Jin H-R, Chi DH, Taylor RS (2004) Characteristics of tissue-engineered cartilage from human auricular chondrocytes. Biomats 25(12):2363–2369

Park SH, Seo JY, Park JY, Ji YB, Kim K, Choi HS, Choi S, Kim JH, Min BH, Kim MS (2019) An injectable, click-crosslinked, cytomodulin-modified hyaluronic acid hydrogel for cartilage tissue engineering. NPG Asia Mater 11(1):1–16

Raisi A, Asefnejad A, Shahali M, Kazerouni ZAS, Kolooshani A, Saber-Samandari S, Moghadas BK, Khandan A (2020) Preparation, characterization, and antibacterial studies of N, O-carboxymethyl chitosan as a wound dressing for bedsore application. Arch Trauma Res 9(4):181–188

Raisi A, Asefnejad A, Shahali M, Doozandeh Z, KamyabMoghadas B, Saber-Samandari S, Khandan A (2022) A soft tissue fabricated using a freeze-drying technique with carboxymethyl chitosan and nanoparticles for promoting effects on wound healing. J Nanoanalysis 7(4):262–274

Razeghian E, Margiana R, Chupradit S, Bokov DO, Abdelbasset WK, Marofi F, Shariatzadeh S, Tosan F, Jarahian M (2021) Mesenchymal stem/stromal cells as a vehicle for cytokine delivery: an emerging approach for tumor immunotherapy. Front Med. https://doi.org/10.3389/fmed.2021.721174

Sahmani S, Saber-Samandari S, Khandan A, Aghdam MM (2019) Nonlinear resonance investigation of nanoclay based bio-nanocomposite scaffolds with enhanced properties for bone substitute applications. J Alloys Compd 773:636–653

Sakaguchi Y, Sekiya I, Yagishita K, Muneta T (2005) Comparison of human stem cells derived from various mesenchymal tissues: superiority of synovium as a cell source. Arthritis Rheum 52(8):2521–2529

Salmani MM, Hashemian M, Khandan A (2020a) Therapeutic effect of magnetic nanoparticles on calcium silicate bioceramic in alternating field for biomedical application. Ceram Int 46(17):27299–27307

Salmani MM, Hashemian M, Yekta HJ, Nejad MG, Saber-Samandari S, Khandan AJJOS, Magnetism N (2020b) Synergic effects of magnetic nanoparticles on hyperthermia-based therapy and controlled drug delivery for bone substitute application. J Supercond Nov Mag 33:2809–2820

Shirani K, Sheikhbahaei E, Torkpour Z, Nejad MG, Moghadas BK, Ghasemi M, Aghdam HA, Ehsani A, Saber-Samandari S, Khandan A (2020) A narrative review of COVID-19: the new pandemic disease. Ir J Med Sci 45(4):233

Sowmya S, Rao RS, Prasad K (2020) Development of clinico-histopathological predictive model for the assessment of metastatic risk of oral squamous cell carcinoma. J Carcinog 19:2

Sun C, Yarmohammadi A, Isfahani RB, Nejad MG, Toghraie D, Fard EK, Saber-Samandari S, Khandan A (2021) Self-healing polymers using electrosprayed microcapsules containing oil: molecular dynamics simulation and experimental studies. J Mol Liq 325:182

Tolou NB, Fathi MH, Monshi A, Mortazavi, VS, Shirani F, Mohammadi M (2013) the effect of adding Tio2 nanoparticles on dental amalgam properties. Iran J Mater Sci Eng 10(2):46–56

Wardani HA, Rahmadi M, Ardianto C, Balan SS, Kamaruddin NS, Khotib J (2019) Development of nonalcoholic fatty liver disease model by high-fat diet in rats. J Basic Clin Physiol Pharm. https://doi.org/10.1515/jbcpp-2019-0258

Yang L, Fattepur S, Nilugal KC, Asmani F, Yusuf E, Ghani MNA, Abdullah I (2018) Neuro-protection of *Abelmoschus esculentus* L. against diabetic neuropathy. Asia J Pharm Clin Res 11(3):28

You SH, Yoon MY, Moon JS (2021) Antioxidant and anti-inflammatory activity study of fulvic acid. J Nat Sci Biol Med 12(3)

Zeylabi A, Shirani F, Heidari F, Farhad AR (2010) Endodontic management of a fused mandibular third molar and distomolar: a case report. Aust Endod J 36(1):29–31